Accepted Manuscript

VP1 crystal structure-guided exploration and optimization of 4,5-dimethoxybenzene-based inhibitors of rhinovirus 14 infection

Laurène Da Costa, Manon Roche, Els Scheers, Antonio Coluccia, Johan Neyts, Thierry Terme, Pieter Leyssen, Romano Silvestri, Patrice Vanelle

PII: S0223-5234(16)30231-8

DOI: 10.1016/j.ejmech.2016.03.049

Reference: EJMECH 8474

To appear in: *European Journal of Medicinal Chemistry*

Received Date: 8 February 2016

Revised Date: 17 March 2016

Accepted Date: 18 March 2016

Please cite this article as: L. Da Costa, M. Roche, E. Scheers, A. Coluccia, J. Neyts, T. Terme, P. Leyssen, R. Silvestri, P. Vanelle, VP1 crystal structure-guided exploration and optimization of 4,5-dimethoxybenzene-based inhibitors of rhinovirus 14 infection, *European Journal of Medicinal Chemistry* (2016), doi: 10.1016/j.ejmech.2016.03.049.

This is a PDF file of an unedited manuscript that has been accepted for publication. As a service to our customers we are providing this early version of the manuscript. The manuscript will undergo copyediting, typesetting, and review of the resulting proof before it is published in its final form. Please note that during the production process errors may be discovered which could affect the content, and all legal disclaimers that apply to the journal pertain.

ACCEPTED MANUSCRIPT

VP1 crystal structure-guided exploration and optimization of 4,5-dimethoxybenzene-based inhibitors of rhinovirus 14 infection

Leave this area blank for abstract info.

Laurène Da Costa,[1] Manon Roche,[1] Els Scheers,[2] Antonio Coluccia,[3] Johan Neyts,[2] Thierry Terme,[1] Pieter Leyssen,[2] Romano Silvestri,[3] and Patrice Vanelle.[1]

[1] *Aix-Marseille Université, Institut de Chimie Radicalaire, UMR 7273 CNRS, 27 Boulevard Jean Moulin, Marseille, France.*

[2] *KU Leuven – University of Leuven, Department of Microbiology and Immunology, Rega Institute for Medical Research, Laboratory of Virology and Chemotherapy, B-3000 Leuven, Belgium.*

[3] *Institut Pasteur Italy, Department of Drug Chemistry and Technologies, Sapienza University, I-00185 Rome, Italy.*

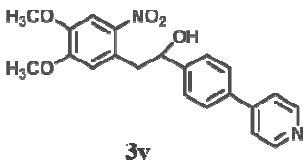

3v

$EC_{50} = 3.4 \pm 1.0\ \mu M$
$CC_{50} > 263\ \mu M$

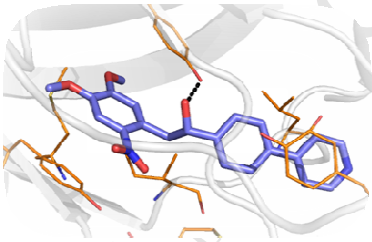

ACCEPTED MANUSCRIPT

ACCEPTED MANUSCRIPT

VP1 crystal structure-guided exploration and optimization of 4,5-dimethoxybenzene-based inhibitors of rhinovirus 14 infection

Laurène Da Costa,[1] Manon Roche,[1] Els Scheers,[2] Antonio Coluccia,[3] Johan Neyts,[2**] Thierry Terme,[1] Pieter Leyssen,[2] Romano Silvestri,[3***] and Patrice Vanelle.[1*]

[1] *Aix-Marseille Université, Institut de Chimie Radicalaire, UMR 7273 CNRS, 27 Boulevard Jean Moulin, Marseille, France.*

[2] *KU Leuven-University of Leuven, Department of Microbiology and Immunology, Rega Institute for Medical Research, Laboratory of Virology and Chemotherapy, B-3000 Leuven, Belgium.*

[3] *Institut Pasteur Italy, Department of Drug Chemistry and Technologies, Sapienza University, I-00185 Rome, Italy.*

** Corresponding author for chemistry. Tel.: +33-4-91835580; fax: 33-4-91-79-46-77; e-mail: patrice.vanelle@univ-amu.fr*

*** Corresponding author for biology. Tel.: +32-16-332883; fax: 32-16-337340; e-mail: johan.neyts@rega.kuleuven.be*

**** Corresponding author for in silico design. Tel.: +39-06-4991-3800; fax: 39-6-4991-3993; e-mail: romano.silvestri@uniroma1.it*

Abstract

Human rhinoviruses (HRV) are the predominant cause of common colds and flu-like illnesses, but are also responsible for virus-induced exacerbations of asthma and chronic obstructive pulmonary disease. However, to date, no drug has been approved yet for clinical use. In this study, we present the results of the structure-based lead optimization of a class of new small-molecule inhibitors that we previously reported to bind into the pocket beneath the canyon of the VP1 protein. A small series of analogues that we designed based on the available structure and interaction data were synthesized and evaluated for their potency to inhibit the replication of HRV serotype 14. 2-(4,5-Dimethoxy-2-nitrophenyl)-1-(4-(pyridin-4-yl)phenyl)ethanol (**3v**) was found to be a potent inhibitor exhibiting micromolar activity (EC_{50} = 3.4 ± 1.0 µM) with a toxicity for HeLa cells that was significantly lower than that of our previous hit (LPCRW_0005, CC_{50} = 104.0 ± 22.2 µM; **3v**, CC_{50} > 263 µM).

Keywords

VP1 protein, HRV14, capsid inhibitors, *in silico* design, TDAE.

1. Introduction

Human rhinoviruses (HRV) are single-stranded, positive-sense RNA viruses that belong to the family of *Picornaviridae*. Based on whole-genome sequencing and taxonomic analysis, these human pathogens can be divided into three genetically distinct HRV groups, designated groups A, B, and C. Each group contains multiple serotypes [1-2]. HRVs are pathogens of the respiratory tract and are a major cause of acute, predominantly mild and self-limiting infections, the so-called "common cold". The incidence of the disease usually dramatically increases during fall, and HRVs are responsible for up to 80% of colds [3]. The clinical symptoms are a runny nose and coughing, and less frequently, wheezing, otitis media, sinusitis, or even pneumonia. Several studies demonstrated that HRVs-induced disease can be more acute in children or immunodeficient patients [4]. Overall, HRV infections have a major economic impact through loss of productivity and strain on the healthcare system. Currently, treatment is limited to symptomatic therapy with over-the-counter medicines. The development of vaccines for prevention is not (yet) an option because of the large number of serotypes [5]. Over recent decades, several small-molecule inhibitors have been developed to treat the common cold caused by rhinovirus infection [6]. However, none of these candidates reached the market, mainly because the side-effects of the treatment did not outweigh the burden of the disease or due to lack of efficacy in clinical studies. Recently, the causative link between rhinovirus infection, exacerbation of asthma and chronic obstructive pulmonary disease (COPD) [7] has triggered, both in academic circles and in pharmaceutical industry, a new interest in the development of an anti-rhinoviral drug [8].

Different stages of the virus replication cycle can be targeted by small-molecule inhibitors. In particular, the capsid protein VP1 has shown promise for the development of antiviral molecules, as it contains a large pocket beneath the receptor-binding canyon [9]. Strikingly, this has led to the discovery and development of a variety of structurally different inhibitors [10]. Our research teams recently reported a novel chemical scaffold of VP1 inhibitors characterized by a 4,5-dimethoxybenzene skeleton [11]. The base structure of this compound class resulted from a synthesis method using Tetrakis(DimethylAmino)Ethylene (TDAE). This is an organic reducing agent [12] which reacts with haloalkyl derivatives to generate an anion under mild conditions *via* two sequential transfers of one electron. This carbanion is able to react with various electrophiles, such as aromatic aldehydes, α-ketoester, α-ketomalonate, α-ketolactam, and sulfonimine derivatives [13-14]. This methodology was used to explore the structure-activity relationships of 4,5-dimethoxybenzene derivatives [11].

From this series, LPCRW_0005 (Figure 1, EC_{50} = 2.2 ± 0.5 µM; CC_{50} = 104.0 ± 22.2 µM) was selected as prototype compound and was, in parallel with pleconaril (Figure 1, EC_{50} = 0.2 ± 0.1 µM; CC_{50} = 50.2 ± 5.0 µM), the subject of a detailed study. We examined its molecular mechanism of action and solved the crystal structure of the compound bound to the VP1 protein (PDB ID: 4PDW) [15].

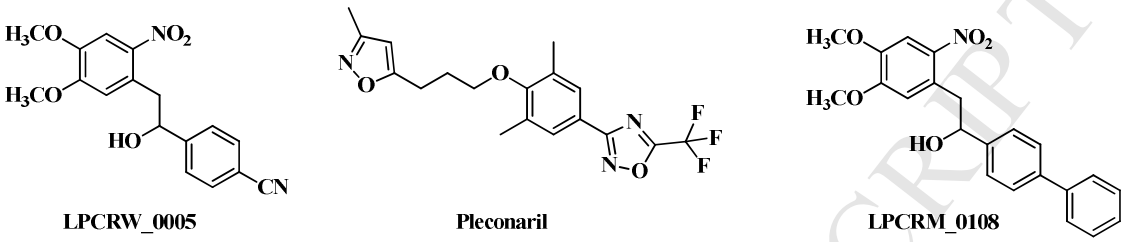

Figure 1. Rhinovirus replication inhibitors.

Several key interactions were identified by superimposition of the binding modes of LPCRW_0005 and pleconaril: (i) the open end of the pocket is left empty by LPCRW_0005; (ii) an extra density was observed in the crystal structure data that could be modelled as a glycerol. Given that pleconaril is a more voluminous compound than LPCRW_0005, it should be possible to manipulate the 4,5-dimethoxybenzene scaffold to optimize the interactions within the drug-binding pocket. Our previous study [11] encouraged this strategy, with LPCRM_0108, which bears a biphenyl group as extra hydrophobic ring (C-ring) (Figure 1, EC_{50} = 1.97 ± 0.10 µM).

Instead of pursuing a solely bio-assay-guided strategy for the further optimization of this compound class, it was decided to make use of the available crystal structure data and to use docking experiments (*in silico* design) to focus the chemistry effort. During this study, the results of which are reported here, five series of potential inhibitors of rhinovirus replication were designed, synthesized, and evaluated for antiviral activity on the replication of rhinovirus in a virus-cell-based assay. The base scaffold and its nomenclature are summarized in Figure 2.

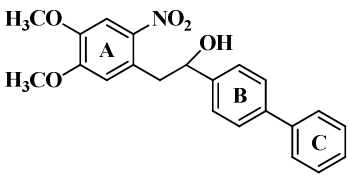

Figure 2. Structure and nomenclature of the 4,5-dimethoxybenzene derivatives investigated in the present study.

2. Results and discussion

2.1. Design strategy

To test the performance of the available *in silico* design platform, we first carried out a cross-docking analysis using PLANTS [16], Glide [17], and Autodock [18] docking algorithms to explore four different HRV14 capsid PDB structures (see Experimental section). The best scoring pose for each docking algorithm was compared with the corresponding crystallographic conformation in terms of the root-mean-square deviation (rmsd) of atomic positions. Given the consistent rmsd values (see Supporting Information), docking experiments were performed by means of PLANTS. The PLANTS LPCRW_0005 binding mode was superimposed on the co-crystallized complex, revealing the same interactions previously reported [15]. Moreover, the docking study led to the identification of other hydrophobic interactions between the A-ring and residues V188 and M224 (Figure 3).

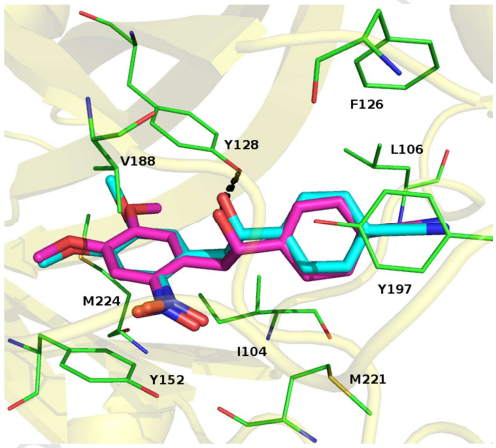

Figure 3. PLANTS binding mode of LPCRW_0005 (magenta) versus co-crystallized binding pose of LPCRW_0005 (cyan). Closest residues are reported as green lines, the rest of the structure of VP1 is shown as ribbons. H-bonds are depicted as dotted black lines.

To complete the model before embarking on to a drug design effort, the binding mode of the active LPCRM_0108 was also studied (Figure 4). This molecule engaged in the same interactions that were observed for LPCRW_0005, but it was also observed that its C-ring engages in additional positive interactions with the hydrophobic pocket. These hydrophobic contacts with L106 and F126, together with a π-π interaction with Y197, are in agreement with the slightly better antiviral activity of LPCRM_0108 as compared to LPCRW_0005.

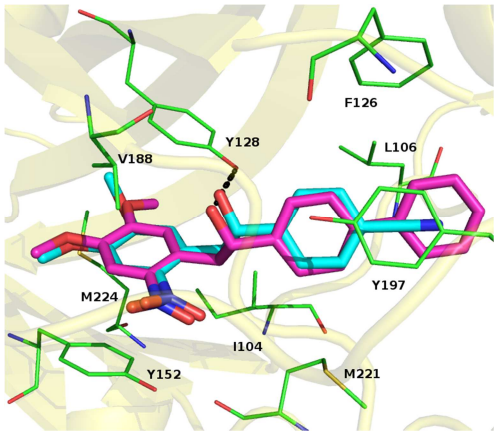

Figure 4. Binding mode of the proposed scaffold (magenta) versus co-crystallized binding pose of LPCRW_0005 (cyan). Closest residues are reported as green lines, the VP1 backbone is shown as a ribbon. H-bonds are depicted as dotted black lines.

To extend the scaffold with an extra hydrophobic residue in an attempt to further improve the antiviral activity, a total of five options were explored: introduction of (i) a *para*-substituted C-ring, (ii) a *meta*-substituted C-ring, (iii) an *ortho*-substituted C-ring, (iv) a *meta*-substituted B-ring by aryl group and, (v) a para-substituted B-ring by heterocycle (Figure 5).

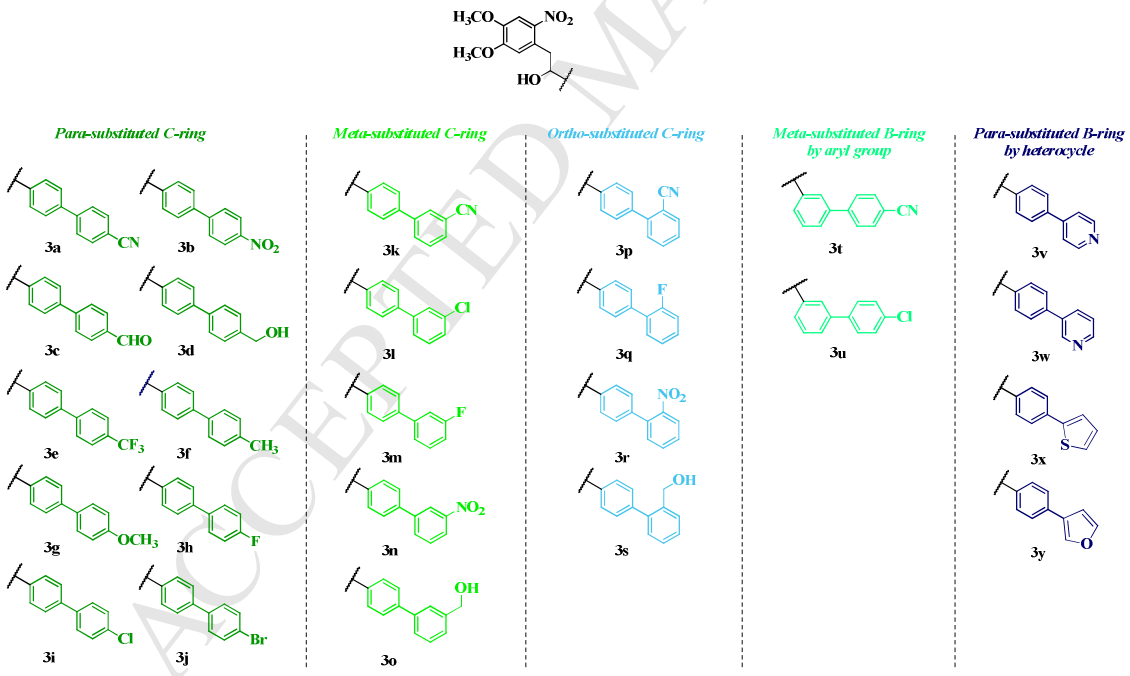

Figure 5. Overview of the modifications proposed during the *in silico*-assisted optimization of the structure-activity relationships.

From the docking experiments, the *para* (**3a-3j**), *meta* (**3k-3o**), and *ortho* (**3p-3s**) -*substituted C-ring* derivatives showed a binding mode consistent with that proposed for the parent compounds (Figure 6A, B and, C). Among the three substitution patterns, the

substituents in *para* position pointed toward the open end of the VP1 pocket (Figure 6A). The substituents in *meta* position filled a hydrophobic pocket formed by L116 and V122, engaging in additional interactions (Figure 6B). Furthermore, the nitro (**3n**) and hydroxymethyl (**3o**) derivatives established a hydrogen bond with L106. The *ortho* substituents appear to lead to non-coplanarity of B- and C-rings, and this might affect the hydrophobic stabilization of the C-ring. It is worth noting that the nitro (**3r**) and hydroxymethyl (**3s**) derivatives established an H-bond with the L106 backbone (Figure 6C).

In contrast, the *meta*-substitution of the B-ring by an aryl group (compounds **3t** and **3u**) induced a completely different binding mode. None of the binding interactions described for LPCRW_0005 could be observed (data not shown). When the C-ring was replaced with a heterocycle (**3v-3y**), the PLANTS proposed binding mode was consistent with that of LPCRW_0005 and all the interactions previously described were maintained. Nevertheless, all heterocycles appear to lead to hydrophobic interactions with Y197 and F126 (Figure 6D).

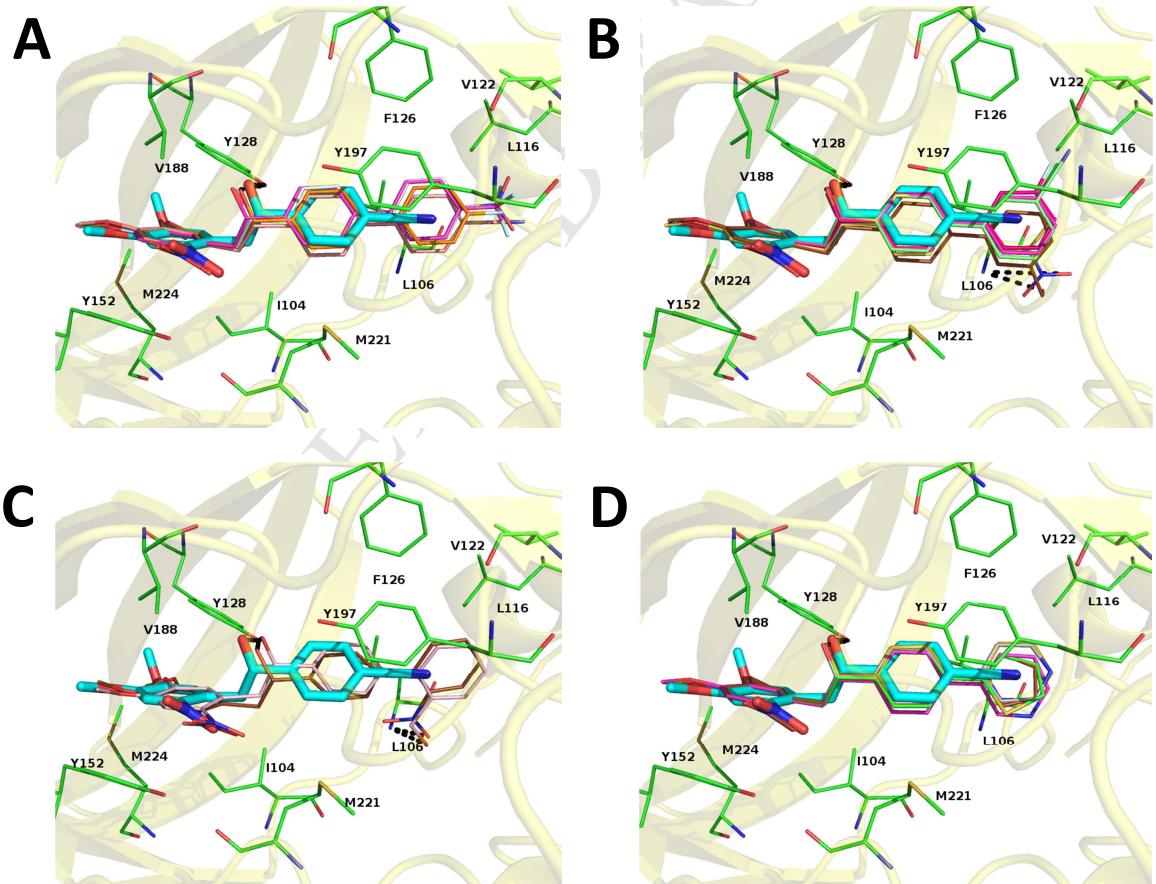

Figure 6. PLANTS binding mode of **Panel A**: *para-substituted C-ring* derivatives **3a** (pink), **3b** (white), **3e** (magenta), and **3h** (orange) versus co-crystallized conformation of LPCRW_0005 (cyan); **Panel B**: *meta-substituted C-ring* derivatives **3k** (green), **3l** (magenta), **3m** (red), **3n** (yellow), and **3o** (brown); **Panel C**: *ortho-substituted C-ring* derivatives **3r** (pink), **3s** (brown); **Panel D**: *heterocycle C-ring* derivatives **3v** (white), **3w** (magenta), **3x** (green), and **3y** (brown). Closest residues are reported as green lines, the VP1 skeleton is shown as ribbon structure. H-bonds are depicted as dotted black lines.

The results of the *in silico* design study were used iteratively with chemistry and biological evaluation rounds to rationalize and focus the chemistry effort in the next step towards the further optimization of the 4,5-dimethoxybenzene derivatives.

2.2. Chemistry

To synthesize the 4,5-dimethoxybenzene derivatives of interest, we followed a synthetic pathway involving two steps: a Suzuki cross-coupling reaction and a nucleophilic addition using TDAE. This synthesis strategy for compounds **3a-3y** is illustrated in Scheme 1.

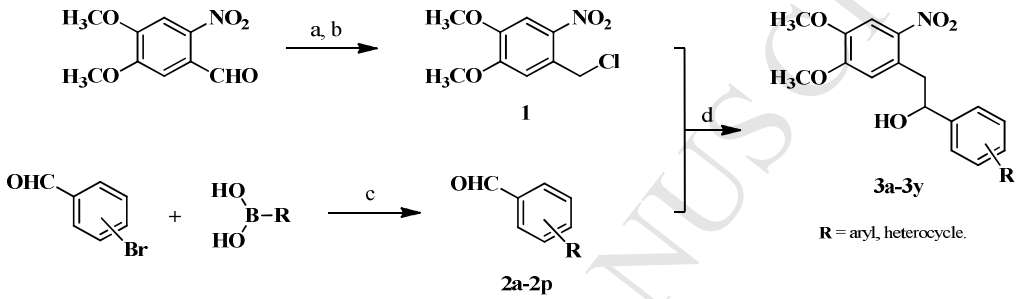

Scheme 1. General pathway for the synthesis of 4,5-dimethoxybenzene derivatives. Reagents and conditions: (a) $NaBH_4$, $MeOH/CH_2Cl_2$, rt, 12 h, 99%; (b) $SOCl_2$, Et_3N, CH_2Cl_2, rt, 12 h, 98%; (c) $Pd(PPh_3)_4$, K_2CO_3, DMF/H_2O, MW (130 °C), 0.5-1 h, 42-99%; (d) TDAE (1.1 equiv.), DMF, *1.* -20 °C, 1 h, *2.* rt, 12 h, 15-92%.

The starting material, 1-(chloromethyl)-4,5-dimethoxy-2-nitrobenzene **1**, was prepared *via* a first reductive reaction followed by chlorination. While, most of the required aromatic aldehydes **2** were commercially, sixteen of them were prepared using a simple cross-coupling aryl-aryl or aryl-heterocycle reaction between a phenylboronic acid and the 3- or 4-bromobenzaldehyde. The use of microwave irradiation allowed us to obtain these compounds **2a-2p** in 42-99% yields.

All compounds (**3a-3y**) of this series were generated by a TDAE-initiated reaction on intermediate **1** with benzaldehyde derivatives under classical TDAE conditions already described [11]. This synthesis strategy involved 3 equiv. of aldehyde in the presence of 1.1 equiv. of TDAE, and allowed us to synthesize the compounds with average yields of 55%.

2.3. *In vitro* evaluation of biological activity

The antiviral activity of all compounds and of the reference compound pleconaril was evaluated in an *in vitro* cytopathic effect reduction (CPE) assay against HRV serotypes 14 (group B rhinoviruses), and 2 (group A rhinoviruses). No activity was observed against HRV

serotype 2 (data not shown). The data for activity against HRV14 are summarized in the tables below.

2.3.1. Para-substituted C-ring

The introduction of a group with either a hydrogen bond acceptor, hydrophobic or hydrophilic properties on the C-ring produced compounds with high cytotoxic properties for HeLa cells. Only compound **3b**, bearing a NO_2 group, proved to only slightly inhibit rhinovirus-induced cell death (**3b**: EC_{50} = 4.7 ± 0.6 µM; CC_{50} = 21.0 ± 6.0 µM). To sum up, the presence of a C-ring substituted in *para*-position induced high toxicity for HeLa cells and did not give rise to compounds with a better antiviral profile than LPCRW_0005 (Table 1).

Table 1. *In vitro* evaluation of the antiviral activity of *para*-substituted C-ring derivatives against HRV14.

Compound	EC_{50} [a, b]	CC_{50} [a, b]	SI
3a	> 4.7	4.7 ± 0.1	ND
3b	4.7 ± 0.6	21.0 ± 6.0	4.5
3c	> 245	> 245	ND
3d	> 244	> 244	ND
3e	> 6.0	4.1 ± 1.3	ND
3f	> 4.7	4.7 ± 0.1	ND
3g	> 244	> 244	ND
3h	> 4.5	4.5 ± 0.3	ND
3i	> 4.1	4.1 ± 0.2	ND
3j	> 4.3	4.3 ± 0.1	ND

EC_{50} = 50% Effective Concentration (concentration at which 50% inhibition of virus-induced cell death is observed).
CC_{50} = 50% Cytostatic/Cytotoxic Concentration (concentration at which 50% adverse effect is observed on host cell viability).
SI = Selectivity Index for HRV14, SI = CC_{50}/EC_{50}.
ND = not determined.
[a] All values are in µM, expressed as median ± Med. Abs. Dev.
[b] In assay conditions: pleconaril EC_{50} = 0.2 ± 0.1 µM; CC_{50} = 50.2 ± 5.0 µM.

2.3.2. Meta-substituted C-ring

The effect of the five substitutions, i.e. CN, NO_2, Cl, F, and a hydroxymethyl group, were also evaluated in the *meta*-position. The presence of a C-3' substitution increased activity (Table 2). In fact, for compounds **3k**, **3l**, and **3o**, EC_{50} values less than 2 µM were observed. However, the extension of the scaffold by introduction of a C-ring substituted in *meta*-position did not reduce the toxicity of these compounds (SI on average of 3.5).

Table 2. *In vitro* evaluation of the antiviral activity of *meta*-substituted C-ring derivatives against HRV14.

Compound	EC_{50} [a, b]	CC_{50} [a, b]	SI
3k	1.4 ± 0.2	5.2 ± 1.0	3.7
3l	1.7 ± 0.1	5.9 ± 1.1	3.5
3m	2.2 ± 0.3	7.4 ± 2.3	3.4
3n	2.2 ± 0.9	5.5 ± 0.7	2.5
3o	1.4 ± 0.4	6.0 ± 1.7	4.3

Legend to the table: see Table 1.

2.3.3. Ortho-substituted C-ring

A smaller series of *ortho*-substituted C-ring derivatives was also explored (Table 3). In contrast to what would be expected from the *in silico* model prediction, compounds **3r** and **3s** revealed an anti-rhinovirus potency similar to that of the *meta*-substituted C-ring (**3r**: EC_{50} = 1.5 ± 0.1 µM; **3s**: EC_{50} = 3.0 ± 0.1 µM) with slightly lower toxicity for HeLa cells.

Table 3. *In vitro* evaluation of the antiviral activity of *ortho*-substituted C-ring derivatives against HRV14.

Compound	EC_{50} [a, b]	CC_{50} [a, b]	SI
3p	> 9.3	9.3 ± 3.6	ND
3q	> 5.0	5.0 ± 2.0	ND
3r	1.5 ± 0.1	9.5 ± 1.9	6.3
3s	3.0 ± 0.1	24.0 ± 2.0	8.0

Legend to the table: see Table 1.

2.3.4. Meta-substituted B-ring by aryl group

In an attempt to further stabilize the interaction of the compounds with the hydrophobic pocket, the influence of a phenyl group in *meta*-position of the B-ring was explored (Table 4). This strategy was quickly abandoned, as no antiviral effect could be observed for any of the compounds for an improvement of the cytotoxicity.

Table 4. *In vitro* evaluation of the antiviral activity of *meta*-substituted B-ring derivatives against HRV14.

Compound	EC_{50} [a, b]	CC_{50} [a, b]	SI
3t	> 9.3	9.3 ± 3.6	ND
3u	> 5.0	5.0 ± 2.0	ND

Legend to the table: see Table 1.

2.3.5. Heterocyclic C-ring

In a fifth series of compounds, we assessed the influence of heterocyclic substituents (i.e. pyridine, furan and thiophene) in *para*-position on B-ring (Table 5). Introduction of a 3- or 4-substituted pyridine (compounds **3v**, and **3w**) yielded compounds with potent antiviral activity. Although the EC_{50} values were similar to those obtained for the compounds reported above (**3v**: EC_{50} = 3.4 ± 1.0 µM; **3w**: EC_{50} = 2.0 ± 0.8 µM), these modifications resulted in a significantly reduced toxic effect on HeLa cells (**3v** and **3w**: CC_{50} > 263 µM). Furthermore, the introduction of thiophene and furan heterocycles improved the antiviral activity to EC_{50} values lower than 2 µM (**3x**: EC_{50} = 1.6 ± 0.2 µM; **3y**: EC_{50} = 1.6 ± 0.2 µM), although the CC_{50} also shifted to lower concentrations, yielding SI values lower than those of **3v** and **3w**. According to the hit selection criteria (i.e. the cell and monolayer morphology of treated, infected cells should, following microscopic inspection, look like uninfected, and untreated control cells), compound **3v** presented, *in vitro*, a promising hit profile.

Table 5. *In vitro* evaluation of the antiviral activity of heterocycle *para*-substituted B-ring derivatives against HRV14.

Compound	EC_{50} [a, b]	CC_{50} [a, b]	SI
3v	3.4 ± 1.0	> 263	77.3
3w	2.0 ± 0.8	> 263	131.5
3x	1.6 ± 0.2	11.0 ± 6.0	6.9
3y	1.6 ± 0.2	5.3 ± 0.1	3.3

Legend: see table 1.

3. Conclusion

In summary, novel 4,5-dimethoxybenzene derivatives were designed to better fills the drug-binding pocket of capsid protein VP1 of HRV serotype 14. Structure-based guided design, efficient synthesis and subsequent evaluation in a virus-cell-based assay led to the discovery of a new and potent inhibitor of rhinovirus replication (**3v**) exhibiting micromolar activity (EC_{50} = 3.4 ± 1.0 µM) and a CC_{50} that is significantly higher than that of our previous hit (LPCRW_0005, CC_{50} = 104.0 ± 22.2 µM; **3v**, CC_{50} > 263 µM).

Follow-up studies will be conducted to explore structure-based strategies with the purpose to broaden the antiviral activity of this compound series to other rhinovirus types.

4. Experimental section

4.1. Molecular Modeling

All molecular modeling studies were performed on a MacPro dual 2.66 GHz Xeon running Ubuntu 12. The HRV capsid structures were downloaded from PDB [20]: 4PDW [15]; 1NCQ [21]; 2HWB [22]; 2HWC [22]; 1R09 [23]. Hydrogen atoms were added to the protein, using Molecular Operating Environment (MOE) 2007.09 [24] and minimized, keeping all the heavy atoms fixed until a rmsd gradient of 0.05 kcal.mol^{-1}.Å^{-1} was reached. Ligand structures were built with MOE and minimized using the MMFF94x force field until a rmsd gradient of 0.05 kcal.mol^{-1}.Å^{-1} was reached. The images depicted in this report were generated by Pymol [25].

4.2. Chemistry

4.2.1. General

Commercially available reagents and solvents were used without further purification. Microwave-assisted reactions were performed in 10-20 mL sealed vials using a Biotage® Initiator Classic Microwave oven; temperatures were measured with an IR-sensor and reaction times are given as hold times. Reactions were monitored by thin-layer chromatography (plates coated with silica gel 60 F_{254} from Merck) and by LC-MS analyses with a Thermo Scientific Accela High Speed LC System® coupled with a single quadrupole mass spectrometer Thermo MSQ Plus®. The RP-HPLC column used is a Thermo Hypersil Gold® 50 x 2.1 mm (C18 bounded), with particles of 1.9 µm diameter. Analysis was 8 min running with a MeOH/H_2O eluent gradient from 50:50 to 95:05. Silica gel 60 (70-230 mesh from Macherey-Nagel) was used for flash chromatography. Melting points were measured in open capillary tubes with Büchi apparatus and are uncorrected. ^{1}H and ^{13}C NMR spectra were recorded at room temperature in deuterated solvents on a Brüker Avance-250 instrument (250 MHz), a Brüker Avance III nanobay-300 MHz or a Brüker Avance III nanobay-400 MHz. Chemical shifts (δ) are reported in parts per million (ppm) relative to TMS as internal standard or relative to the solvent [^{1}H: δ(DMSO) = 2.50 ppm, δ($CDCl_3$) = 7.26 ppm; ^{13}C δ(DMSO) = 39.52 ppm, δ($CDCl_3$) = 77.16 ppm]. Data are reported as follows: chemical shift, multiplicity (s = singulet, d = doublet, t = triplet, q = quartet, dd = doublet of doublets, and m = multiplet), coupling constant in Hertz, and integration. Two-dimensional spectroscopy (HSQC and HMBC) was used to assist in the assignment and the data are not reported.

Elemental analyses were carried out at the Spectropole, Faculté des Sciences de Saint Jérôme, Marseille (France) and accurate mass measurements (HRMS) were recorded on a TOF spectrometer, realized by Spectropole of Faculté des Sciences de Saint Jérôme, Marseille (France).

4.2.2. *1-(Chloromethyl)-4,5-dimethoxy-2-nitrobenzene (**1**)*

Step (a): To a solution of a 6-nitroveratraldehyde (20.0 g, 95 mmol) in a mixture of MeOH/CH_2Cl_2 (800 mL; 3:1), $NaBH_4$ (7.6 g, 199 mmol) was slowly added at 0 °C. After stirring overnight at room temperature, the reaction was quenched by addition of water. The organic layer was washed with water and brine, dried over Na_2SO_4, filtered off and concentrated under reduced pressure. After purification by column chromatography on silica gel (CH_2Cl_2), the pure product (4,5-dimethoxy-2-nitrophenyl)methanol (19.7 g, 92 mmol) was obtained as a yellow solid. Yield, *99%*.

Step (b): To a solution of (4,5-dimethoxy-2-nitrophenyl)methanol (19.5 g, 91 mmol) in CH_2Cl_2 (55 mL) was added a few drops of triethylamine, and $SOCl_2$ (1.3 mL, 18 mmol) at 0 °C. After stirring overnight at room temperature, the reaction was quenched by addition of EtOH. The organic layer was washed with water and brine, dried over Na_2SO_4, filtered off and concentrated under reduced pressure. After purification by column chromatography on silica gel (Cyclohexane/EtOAc 7:3), the pure product **1** (20.7 g, 90 mmol) was obtained as a yellow solid. Yield, *98%*. m.p: 59.9 °C. ^{1}H NMR (250 MHz, $CDCl_3$) δ 7.68 (s, 1H), 7.09 (s, 1H), 5.00 (s, 2H), 4.00 (s, 3H), 3.96 (s, 3H). ^{13}C NMR (100 MHz, $CDCl_3$) δ 153.5, 148.8, 140.4, 127.3, 112.9, 108.5, 56.6, 56.5, 43.7.

4.2.3. *General procedure **A** for Suzuki cross-coupling reactions*

To a solution of a 3- or 4-bromobenzaldehyde in a mixture DMF/water (3:1; 14.8 mL/mmol) were added boronic acid derivative (1.5 equiv.), $Pd(PPh_3)_4$ (5 mol%), and K_2CO_3 (2 equiv.). The reaction mixture was heated under microwave irradiation (130 °C) until TLC showed complete conversion of the starting material (0.5-1 h). After cooling, the mixture was extracted with dichloromethane. The combined organic layers were washed with water and brine, dried over Na_2SO_4, filtered off, and concentrated under reduced pressure to afford the corresponding crude product **2**.

Compounds **2a-2p** were synthesized following the procedure described above from the corresponding boronic acids.

4.2.4. *General procedure **B** for TDAE reaction with various electrophiles*

To a glass vessel capable of being sealed with Teflon cap (for microwave vials) were added **1** and benzaldehyde derivative (3 equiv.). The vessel was capped and then, evacuated and backfilled with N_2 (process repeated 3X). Anhydrous DMF (3.5 mL/mmol) was introduced and the solution was vigorously stirred for 20 min at -20 °C. TDAE was added slowly and the mixture was stirred for one hour. Then, the reaction was stirred at room temperature overnight. After LC-MS analysis clearly showed that the chloride had been totally consumed, the reaction was hydrolysed with distilled water. The mixture was then extracted with dichloromethane. The combined organic layers were washed with water and brine, dried over Na_2SO_4, filtered off and concentrated under reduced pressure to afford the corresponding crude product **3**.

4.2.4.1. *4'-(2-(4,5-Dimethoxy-2-nitrophenyl)-1-hydroxyethyl)-[1,1'-biphenyl]-4-carbonitrile* (**3a**). The crude product was prepared according to procedure **B** starting from **1** (112 mg, 0.49 mmol) and 4'-formyl-[1,1'-biphenyl]-4-carbonitrile (301 mg, 1.45 mmol). After purification by column chromatography on silica gel (CH_2Cl_2/EtOAc 9:1), the pure product (93 mg, 0.23 mmol) was obtained as a yellow solid. Yield, *48%*. m.p: 185 °C; ^{1}H NMR (400 MHz, DMSO-d_6) δ 7.91 (d, *J* = 8.6 Hz, 2H), 7.87 (d, *J* = 8.6 Hz, 2H), 7.72 (d, *J* = 8.3 Hz, 2H), 7.55 (s, 1H), 7.46 (d, *J* = 8.3 Hz, 2H), 6.87 (s, 1H), 5.47 (d, *J* = 5.0 Hz, 1H), 4.87-4.82 (m, 1H), 3.83 (s, 3H), 3.76 (s, 3H), 3.26 (dd, *J* = 13.2, 4.6 Hz, 1H), 3.18 (dd, *J* = 13.2, 8.4 Hz, 1H). ^{13}C NMR (75 MHz, DMSO-d_6) δ 152.1, 147.0, 146.1, 144.5, 141.7, 136.9, 132.9 (2C), 128.3, 127.4 (2C), 126.8 (2C), 126.6 (2C), 118.9, 115.4, 109.9, 107.9, 72.3, 56.0 (2C), 42.3. Anal. Calcd. for $C_{23}H_{20}N_2O_5$ (%): C, 68.31; H, 4.98; N, 6.93. Found (%): C, 67.79; H, 4.89; N, 6.76.

4.2.4.2. *2-(4,5-Dimethoxy-2-nitrophenyl)-1-(4'-nitro-[1,1'-biphenyl]-4-yl)ethanol* (**3b**). The crude product was prepared according to procedure **B** starting from **1** (78 mg, 0.34 mmol) and 4'-nitro-[1,1'-biphenyl]-4-carbaldehyde **2a** (200 mg, 0.88 mmol). After purification by column chromatography on silica gel (CH_2Cl_2/EtOAc 9:1), the pure product (73 mg, 0.17 mmol) was obtained as a yellow solid. Yield, *51%*. m.p: 202 °C; ^{1}H NMR (250 MHz, DMSO-d_6) δ 8.30 (d, *J* = 8.9 Hz, 2H), 7.96 (d, *J* = 8.9 Hz, 2H), 7.77 (d, *J* = 8.3 Hz, 2H), 7.55 (s, 1H), 7.48 (d, *J* = 8.3 Hz, 2H), 6.88 (s, 1H), 5.51 (d, *J* = 4.9 Hz, 1H), 4.88-4.81 (m, 1H), 3.83 (s, 3H), 3.76 (s, 3H), 3.30-3.14 (m, 2H). ^{13}C NMR (75 MHz, DMSO-d_6) δ 152.5, 147.4, 147.0, 146.9, 146.9, 142.1, 136.9, 128.7, 128.1 (2C), 127.4 (2C), 127.1 (2C), 124.6 (2C), 115.8,

108.3, 72.7, 56.4 (2C), 42.7. Anal. Calcd. for $C_{22}H_{20}N_2O_7$ (%): C, 62.26; H, 4.75; N, 6.60. Found (%): C, 62.28; H, 4.70; N, 6.51.

4.2.4.3. *4'-(2-(4,5-Dimethoxy-2-nitrophenyl)-1-hydroxyethyl)-[1,1'-biphenyl]-4-carbaldehyde* (**3c**). The crude product was prepared according to procedure **B** starting from **1** (74 mg, 0.32 mmol) and [1,1'-biphenyl]-4,4'-dicarbaldehyde **2b** (200 mg, 0.95 mmol). After purification by column chromatography on silica gel (CH_2Cl_2/EtOAc 9:1), the pure product (80 mg, 0.20 mmol) was obtained as a yellow solid. Yield, *62%*. m.p: 163 °C; ^{1}H NMR (250 MHz, DMSO-d_6) δ 10.05 (s, 1H), 7.99 (d, *J* = 8.4 Hz, 2H), 7.81 (d, *J* = 8.4 Hz, 2H), 7.75 (d, *J* = 8.3 Hz, 2H), 7.55 (s, 1H), 7.46 (d, *J* = 8.3 Hz, 2H), 6.87 (s, 1H), 5.49 (d, *J* = 4.9 Hz, 1H), 4.87-4.80 (m, 1H), 3.83 (s, 3H), 3.76 (s, 3H), 3.30-3.14 (m, 2H). ^{13}C NMR (75 MHz, DMSO-d_6) δ 192.7, 152.1, 147.0, 145.9, 145.7, 141.7, 137.4, 135.0, 130.1 (2C), 128.3, 127.2 (2C), 126.8 (2C), 126.5 (2C), 115.3, 107.9, 72.3, 55.9 (2C), 42.3. Anal. Calcd. for $C_{23}H_{21}NO_6$ (%): C, 67.80; H, 5.20; N, 3.44. Found (%): C, 67.34; H, 5.14; N, 3.39.

4.2.4.4. *2-(4,5-Dimethoxy-2-nitrophenyl)-1-(4'-(hydroxymethyl)-[1,1'-biphenyl]-4-yl)ethanol* (**3d**). The crude product was prepared according to procedure **B** starting from **1** (152 mg, 0.65 mmol) and 4'-(hydroxymethyl)-[1,1'-biphenyl]-4-carbaldehyde **2c** (418 mg, 1.97 mmol). After purification by column chromatography on silica gel (CH_2Cl_2/EtOAc 8:2), the pure product (39 mg, 0.09 mmol) was obtained as a light yellow solid. Yield, *15%*. m.p: 180 °C; ^{1}H NMR (250 MHz, DMSO-d_6) δ 7.61 (d, *J* = 8.1 Hz, 4H), 7.55 (s, 1H), 7.39 (d, *J* = 8.1, 4H), 6.84 (s, 1H), 5.41 (d, *J* = 4.9 Hz, 1H), 5.21 (t, *J* = 5.7 Hz, 1H), 4.84-4.77 (m, 1H), 4.53 (d, *J* = 5.7 Hz, 2H), 3.83 (s, 3H), 3.75 (s, 3H), 3.29-3.14 (m, 2H). ^{13}C NMR (100 MHz, DMSO-d_6) δ 152.0, 146.9, 144.5, 141.6 (2C), 138.7, 138.4, 128.4, 127.0 (2C), 126.4 (2C), 126.2 (2C), 126.1 (2C), 115.3, 107.8, 72.4, 62.6, 55.9 (2C), 42.4. Anal. Calcd. for $C_{23}H_{23}NO_6$ (%): C, 67.47; H, 5.66; N, 3.42. Found (%): C, 66.94; H, 5.68; N, 3.23.

4.2.4.5. *2-(4,5-Dimethoxy-2-nitrophenyl)-1-(4'-(trifluoromethyl)-[1,1'-biphenyl]-4-yl)ethanol* (**3e**). The crude product was prepared according to procedure **B** starting from **1** (62 mg, 0.27 mmol) and 4'-(trifluoromethyl)-[1,1'-biphenyl]-4-carbaldehyde **2d** (200 mg, 0.80 mmol). After purification by column chromatography on silica gel (CH_2Cl_2/EtOAc 9:1), the pure product (109 mg, 0.24 mmol) was obtained as a white solid. Yield, *92%*. m.p: 134 °C; ^{1}H NMR (250 MHz, DMSO-d_6) δ 7.89 (d, *J* = 8.2 Hz, 2H), 7.81 (d, *J* = 8.2 Hz, 2H), 7.71 (d, *J* = 8.1 Hz, 2H), 7.55 (s, 1H), 7.45 (d, *J* = 8.1 Hz, 2H), 6.86 (s, 1H), 5.48 (d, *J* = 4.9 Hz, 1H), 4.87-4.80 (m, 1H), 3.83 (s, 3H), 3.76 (s, 3H), 3.30-3.14 (m, 2H). ^{13}C NMR (100 MHz,

DMSO-d_6) δ 152.0, 146.9, 145.8, 144.0, 141.6, 137.2, 128.3, 127.7 (q, *J* = 32 Hz, 1C), 127.3 (2C), 126.7 (2C), 126.5 (2C), 125.7 (q, *J* = 4 Hz, 2C), 124.4 (q, *J* = 270 Hz, 1C), 115.3, 107.8, 72.3, 55.9 (2C), 42.4. Anal. Calcd. for $C_{23}H_{20}F_3NO_5$ (%): C, 61.74; H, 4.51; N, 3.13. Found (%): C, 61.31; H, 4.43; N, 3.07.

4.2.4.6. *2-(4,5-Dimethoxy-2-nitrophenyl)-1-(4'-methyl-[1,1'-biphenyl]-4-yl)ethanol* (**3f**). The crude product was prepared according to procedure **B** starting from **1** (77 mg, 0.33 mmol) and 4'-methyl-[1,1'-biphenyl]-4-carbaldehyde (196 mg, 0.99 mmol). After purification by column chromatography on silica gel (CH_2Cl_2/EtOAc 9:1), the pure product (70 mg, 0.18 mmol) was obtained as a yellow solid. Yield, *54%*. m.p: 109 °C; ^{1}H NMR (250 MHz, DMSO-d_6) δ 7.59 (d, *J* = 8.2 Hz, 2H), 7.54 (d, *J* = 8.0 Hz, 2H), 7.54 (s, 1H), 7.37 (d, *J* = 8.2 Hz, 2H), 7.25 (d, *J* = 8.0 Hz, 2H), 6.83 (s, 1H), 5.41 (d, *J* = 4.8 Hz, 1H), 4.83-4.76 (m, 1H), 3.82 (s, 3H), 3.74 (s, 3H), 3.27-3.12 (m, 2H), 2.33 (s, 3H). ^{13}C NMR (75 MHz, DMSO-d_6) δ 152.0, 146.9, 144.3, 141.7, 138.7, 137.2, 136.6, 129.5 (2C), 128.4, 126.4 (2C), 126.3 (2C), 126.0 (2C), 115.3, 107.8, 72.4, 55.9, 55.9, 42.4, 20.6. Anal. Calcd. for $C_{23}H_{23}NO_5$ (%): C, 70.21; H, 5.89; N, 3.56. Found (%): C, 70.16; H, 6.16; N, 3.39.

4.2.4.7. *2-(4,5-Dimethoxy-2-nitrophenyl)-1-(4'-methoxy-[1,1'-biphenyl]-4-yl)ethanol* (**3g**). The crude product was prepared according to procedure **B** starting from **1** (55 mg, 0.24 mmol) and 4'-methoxy-[1,1'-biphenyl]-4-carbaldehyde (152 mg, 0.71 mmol). After purification by column chromatography on silica gel (CH_2Cl_2/EtOAc 9:1), the pure product (62 mg, 0.15 mmol) was obtained as an off-white solid. Yield, *64%*. m.p: 137 °C; ^{1}H NMR (250 MHz, DMSO-d_6) δ 7.59 (d, *J* = 8.8 Hz, 2H), 7.57 (d, *J* = 8.2 Hz, 2H), 7.55 (s, 1H), 7.37 (d, *J* = 8.2 Hz, 2H), 7.02 (d, *J* = 8.8 Hz, 2H), 6.84 (s, 1H), 5.41 (d, *J* = 4.7 Hz, 1H), 4.83-4.76 (m, 1H), 3.82 (s, 3H), 3.79 (s, 3H), 3.75 (s, 3H), 3.28-3.13 (m, 2H). ^{13}C NMR (62.5 MHz, DMSO-d_6) δ 158.7, 152.0, 146.9, 143.6, 141.6, 138.3, 132.3, 128.2, 127.3 (2C), 126.1 (2C), 125.5 (2C), 115.3, 114.2 (2C), 108.0, 72.2, 55.9, 55.8, 55.0, 42.1. Anal. Calcd. for $C_{23}H_{23}NO_6$ (%): C, 67.47; H, 5.66; N, 3.42. Found (%): C, 67.57; H, 5.73; N, 3.37.

4.2.4.8. *2-(4,5-Dimethoxy-2-nitrophenyl)-1-(4'-fluoro-[1,1'-biphenyl]-4-yl)ethanol* (**3h**). The crude product was prepared according to procedure **B** starting from **1** (104 mg, 0.45 mmol) and 4'-fluoro-[1,1'-biphenyl]-4-carbaldehyde (270 mg, 1.35 mmol). After purification by column chromatography on silica gel (CH_2Cl_2/EtOAc 9:1), the pure product (100 mg, 0.25 mmol) was obtained as a yellow solid. Yield, *56%*. m.p: 131 °C; ^{1}H NMR (250 MHz, DMSO-d_6) δ 7.68 (dd, J_{HH} = 8.9 Hz, J_{HF} = 5.5 Hz, 2H), 7.59 (d, *J* = 8.2 Hz, 2H), 7.54 (s, 1H), 7.39 (d,

J = 8.2 Hz, 2H), 7.27 (dd, J_{HH} = 8.9 Hz, J_{HF} = 8.9 Hz, 2H), 6.84 (s, 1H), 5.42 (d, *J* = 4.9 Hz, 1H), 4.83-4.76 (m, 1H), 3.81 (s, 3H), 3.75 (s, 3H), 3.27-3.12 (m, 2H). ^{13}C NMR (75 MHz, DMSO-d_6) δ 162.2 (d, *J* = 242 Hz, 1C), 152.3, 147.2, 144.7, 141.9, 138.1, 136.7 (d, *J* = 3 Hz, 1C), 128.8 (d, *J* = 8 Hz, 2C), 128.6, 126.7 (2C), 126.5 (2C), 115.9 (d, *J* = 21 Hz, 2C), 115.6, 108.1, 72.6, 56.2 (2C), 42.5. Anal. Calcd. for $C_{22}H_{20}FNO_5$ (%): C, 66.49; H, 5.07; N, 3.52. Found (%): C, 67.10; H, 4.89; N, 3.42.

4.2.4.9. *1-(4'-Chloro-[1,1'-biphenyl]-4-yl)-2-(4,5-dimethoxy-2-nitrophenyl)ethanol* (**3i**). The crude product was prepared according to procedure **B** starting from **1** (107 mg, 0.46 mmol) and 4'-chloro-[1,1'-biphenyl]-4-carbaldehyde (300 mg, 1.38 mmol). After purification by column chromatography on silica gel (CH_2Cl_2/EtOAc 9:1), the pure product (75 mg, 0.18 mmol) was obtained as a yellow solid. Yield, *40%*. m.p: 145 °C; ^{1}H NMR (250 MHz, DMSO-d_6) δ 7.69 (d, *J* = 8.5 Hz, 2H), 7.63 (d, *J* = 8.2 Hz, 2H), 7.55 (s, 1H), 7.51 (d, *J* = 8.5 Hz, 2H), 7.41 (d, *J* = 8.2 Hz, 2H), 6.86 (s, 1H), 5.45 (d, *J* = 4.9 Hz, 1H), 4.85-4.78 (m, 1H), 3.83 (s, 3H), 3.76 (s, 3H), 3.29-3.13 (m, 2H). ^{13}C NMR (75 MHz, DMSO-d_6) δ 152.0, 146.9, 145.1, 141.7, 138.8, 137.4, 132.1, 128.8 (2C), 128.3, 128.3 (2C), 126.4 (2C), 126.2 (2C), 115.3, 107.9, 72.3, 55.9 (2C), 42.3. Anal. Calcd. for $C_{22}H_{20}ClNO_5$ (%): C, 63.85; H, 4.87; N, 3.38. Found (%): C, 63.97; H, 4.72; N, 3.40. HRMS (ESI+) m/z Calc. for $C_{22}H_{20}ClNO_5$ $[M + Na]^+$ 436.0922, found 436.0923.

4.2.4.10. *1-(4'-Bromo-[1,1'-biphenyl]-4-yl)-2-(4,5-dimethoxy-2-nitrophenyl)ethanol* (**3j**). The crude product was prepared according to procedure **B** starting from **1** (95 mg, 0.41 mmol) and 4'-bromo-[1,1'-biphenyl]-4-carbaldehyde **2e** (320 mg, 1.22 mmol). After purification by column chromatography on silica gel (CH_2Cl_2/EtOAc 9:1), the pure product (115 mg, 0.25 mmol) was obtained as a yellow solid. Yield, *62%*. m.p: 119 °C; ^{1}H NMR (250 MHz, DMSO-d_6) δ 7.68-7.60 (m, 6H), 7.56 (s, 1H), 7.42 (d, *J* = 8.2 Hz, 2H), 6.86 (s, 1H), 5.45 (d, *J* = 4.9 Hz, 1H), 4.86-4.79 (m, 1H), 3.83 (s, 3H), 3.76 (s, 3H), 3.29-3.14 (m, 2H). ^{13}C NMR (100 MHz, DMSO-d_6) δ 152.0, 146.9, 145.2, 141.6, 139.2, 137.5, 131.8 (2C), 128.7 (2C), 128.4, 126.5 (2C), 126.2 (2C), 120.7, 115.3, 107.8, 72.3, 55.9 (2C), 42.4. HRMS (ESI+) m/z Calc. for $C_{22}H_{20}BrNO_5$ $[M + Na]^+$ 480.0417, found 480.0418.

4.2.4.11. *4'-(2-(4,5-Dimethoxy-2-nitrophenyl)-1-hydroxyethyl)-[1,1'-biphenyl]-3-carbonitrile* (**3k**). The crude product was prepared according to procedure **B** starting from **1** (101 mg, 0.44 mmol) and 4'-formyl-[1,1'-biphenyl]-3-carbonitrile (272 mg, 1.31 mmol). After purification by column chromatography on silica gel (CH_2Cl_2/EtOAc 9:1), the pure product (102 mg, 0.25

mmol) was obtained as a yellow solid. Yield, *58%*. m.p: 144 °C; ^{1}H NMR (250 MHz, DMSO-d_6) δ 8.15 (s, 1H), 8.04-8.01 (m, 1H), 7.84-7.80 (m, 1H), 7.72 (d, *J* = 8.2 Hz, 2H), 7.70-7.63 (m, 1H), 7.55 (s, 1H), 7.44 (d, *J* = 8.2 Hz, 2H), 6.88 (s, 1H), 5.46 (d, *J* = 4.9 Hz, 1H), 4.87-4.80 (m, 1H), 3.83 (s, 3H), 3.77 (s, 3H), 3.33-3.13 (m, 2H). ^{13}C NMR (100 MHz, DMSO-d_6) δ 152.0, 146.9, 145.8, 141.6, 141.1, 136.6, 131.4, 130.9, 130.2, 130.1, 128.4, 126.6 (2C), 126.5 (2C), 118.8, 115.3, 112.1, 107.8, 72.3, 56.0, 55.9, 42.4. Anal. Calcd. for $C_{23}H_{20}N_2O_5$ (%): C, 68.31; H, 4.98; N, 6.93. Found (%): C, 68.30; H, 4.93; N, 6.76.

4.2.4.12. *1-(3'-Chloro-[1,1'-biphenyl]-4-yl)-2-(4,5-dimethoxy-2-nitrophenyl)ethanol* (**3l**). The crude product was prepared according to procedure **B** starting from **1** (89 mg, 0.38 mmol) and 3'-chloro-[1,1'-biphenyl]-4-carbaldehyde (250 mg, 1.15 mmol). After purification by column chromatography on silica gel (CH_2Cl_2/EtOAc 9:1), the pure product (79 mg, 0.19 mmol) was obtained as a light yellow solid. Yield, *50%*. m.p: 105 °C; ^{1}H NMR (250 MHz, DMSO-d_6) δ 7.71-7.62 (m, 4H), 7.55 (s, 1H), 7.52-7.40 (m, 4H), 6.87 (s, 1H), 5.44 (d, *J* = 4.9 Hz, 1H), 4.86-4.79 (m, 1H), 3.83 (s, 3H), 3.76 (s, 3H), 3.26-3.16 (m, 2H). ^{13}C NMR (75 MHz, DMSO-d_6) δ 152.0, 146.9, 145.5, 142.2, 141.7, 137.2, 133.8, 130.8, 128.4, 127.2, 126.5 (2C), 126.5 (2C), 126.3, 125.3, 115.3, 107.8, 72.3, 55.9 (2C), 42.4. Anal. Calcd. for $C_{22}H_{20}ClNO_5$ (%): C, 63.85; H, 4.87; N, 3.38. Found (%): C, 64.09; H, 4.87; N, 3.84.

4.2.4.13. *2-(4,5-Dimethoxy-2-nitrophenyl)-1-(3'-fluoro-[1,1'-biphenyl]-4-yl)ethanol* (**3m**). The crude product was prepared according to procedure **B** starting from **1** (66 mg, 0.28 mmol) and 3'-fluoro-[1,1'-biphenyl]-4-carbaldehyde (170 mg, 0.85 mmol). After purification by column chromatography on silica gel (CH_2Cl_2/EtOAc 9:1), the pure product (79 mg, 0.20 mmol) was obtained as a white solid. Yield, *70%*. m.p: 89 °C; ^{1}H NMR (300 MHz, DMSO-d_6) δ 7.67 (d, *J* = 8.2 Hz, 2H), 7.55 (s, 1H), 7.52-7.48 (m, 3H), 7.42 (d, *J* = 8.2 Hz, 2H), 7.20-7.15 (m, 1H), 6.86 (s, 1H), 5.40 (d, *J* = 4.8 Hz, 1H), 4.86-4.80 (m, 1H), 3.83 (s, 3H), 3.77 (s, 3H), 3.25-3.15 (m, 2H). ^{13}C NMR (75 MHz, DMSO-d_6) δ 162.7 (d, *J* = 241 Hz, 1C), 152.0, 146.9, 145.3, 142.4 (d, *J* = 8 Hz, 1C), 141.6, 137.3, 130.8 (d, *J* = 8 Hz, 1C), 128.3, 126.4 (4C), 122.5 (d, *J* = 3Hz, 1C), 115.3, 114.9 (d, *J* = 20 Hz, 1C), 113.2 (d, *J* = 22 Hz, 1C), 107.8, 72.2, 55.9 (2C), 42.3. HRMS (ESI+) m/z Calc. for $C_{22}H_{20}FNO_5$ $[M + Na]^+$ 420.1218, found 420.1219.

4.2.4.14. *2-(4,5-Dimethoxy-2-nitrophenyl)-1-(3'-nitro-[1,1'-biphenyl]-4-yl)ethanol* (**3n**). The crude product was prepared according to procedure **B** starting from **1** (101 mg, 0.44 mmol) and 3'-nitro-[1,1'-biphenyl]-4-carbaldehyde **2f** (300 mg, 1.32 mmol). After purification by

column chromatography on silica gel (CH_2Cl_2/EtOAc 9:1), the pure product (120 mg, 0.28 mmol) was obtained as a yellow solid. Yield, *65%*. m.p: 163 °C; ^{1}H NMR (250 MHz, DMSO-d_6) δ 8.43 (s, 1H), 8.23-8.14 (m, 2H), 7.78-7.73 (m, 3H), 7.55 (s, 1H), 7.47 (d, *J* = 8.1 Hz, 2H), 6.89 (s, 1H), 5.48 (d, *J* = 4.9 Hz, 1H), 4.88-4.81 (m, 1H), 3.83 (s, 3H), 3.77 (s, 3H), 3.31-3.14 (m, 2H). ^{13}C NMR (75 MHz, DMSO-d_6) δ 152.0, 148.5, 146.9, 146.0, 141.7, 141.6, 136.4, 133.1, 130.5, 128.3, 126.7 (2C), 126.6 (2C), 122.0, 120.9, 115.3, 107.8, 72.3, 56.0, 55.9, 42.4. Anal. Calcd. for $C_{22}H_{20}N_2O_7$ (%): C, 62.26; H, 4.75; N, 6.60. Found (%): C, 62.25; H, 4.64; N, 6.53.

4.2.4.15. *2-(4,5-Dimethoxy-2-nitrophenyl)-1-(3'-(hydroxymethyl)-[1,1'-biphenyl]-4-yl)ethanol* (**3o**). The crude product was prepared according to procedure **B** starting from **1** (90 mg, 0.39 mmol) and 3'-(hydroxymethyl)-[1,1'-biphenyl]-4-carbaldehyde **2g** (248 mg, 1.17 mmol). After purification by column chromatography on silica gel (CH_2Cl_2/EtOAc 8:2), the pure product (73 mg, 0.18 mmol) was obtained as a yellow solid. Yield, *46%*. m.p: 173 °C; ^{1}H NMR (250 MHz, DMSO-d_6) δ 7.63-7.60 (m, 3H), 7.55 (s, 1H), 7.53-7.50 (m, 1H), 7.42-7.37 (m, 3H), 7.31-7.28 (m, 1H), 6.84 (s, 1H), 5.42 (d, *J* = 4.8 Hz, 1H), 5.24 (t, *J* = 5.8 Hz, 1H), 4.85-4.78 (m, 1H), 4.56 (d, *J* = 5.2 Hz, 2H), 3.82 (s, 3H), 3.75 (s, 3H), 3.29-3.14 (m, 2H). ^{13}C NMR (100 MHz, DMSO-d_6) δ 152.0, 146.9, 144.6, 143.2, 141.7, 139.8, 139.0, 128.7, 128.4, 126.4 (2C), 126.3 (2C), 125.4, 124.9, 124.6, 115.3, 107.8, 72.4, 62.9, 55.9 (2C), 42.4. Anal. Calcd. for $C_{23}H_{23}NO_6$ (%): C, 67.47; H, 5.66; N, 3.42. Found (%): C, 67.04; H, 5.59; N, 3.62.

4.2.4.16. *4'-(2-(4,5-Dimethoxy-2-nitrophenyl)-1-hydroxyethyl)-[1,1'-biphenyl]-2-carbonitrile* (**3p**). The crude product was prepared according to procedure **B** starting from **1** (71 mg, 0.31 mmol) and 4'-formyl-[1,1'-biphenyl]-2-carbonitrile **2h** (190 mg, 0.92 mmol). After purification by column chromatography on silica gel (CH_2Cl_2/EtOAc 9:1), the pure product (63 mg, 0.16 mmol) was obtained as a white solid. Yield, *51%*. m.p: 120 °C; ^{1}H NMR (300 MHz, DMSO-d_6) δ 7.95-7.92 (m, 1H), 7.82-7.77 (m, 1H), 7.62-7.54 (m, 5H), 7.48 (d, *J* = 8.2 Hz, 2H), 6.85 (s, 1H), 5.47 (d, *J* = 4.8 Hz, 1H), 4.89-4.84 (m, 1H), 3.83 (s, 3H), 3.77 (s, 3H), 3.27-3.17 (m, 2H). ^{13}C NMR (75 MHz, DMSO-d_6) δ 152.0, 146.9, 146.0, 144.4, 141.6, 136.4, 133.8, 133.4, 130.0, 128.3 (2C), 128.2, 128.0, 126.1 (2C), 118.5, 115.3, 110.1, 107.9, 72.3, 56.0, 55.9, 42.2. Anal. Calcd. for $C_{23}H_{20}N_2O_5$ (%): C, 68.31; H, 4.98; N, 6.93. Found (%): C, 68.07; H, 4.86; N, 6.85.

4.2.4.17. *2-(4,5-Dimethoxy-2-nitrophenyl)-1-(2'-fluoro-[1,1'-biphenyl]-4-yl)ethanol* (**3q**). The crude product was prepared according to procedure **B** starting from **1** (123 mg, 0.53 mmol)

and 2'-fluoro-[1,1'-biphenyl]-4-carbaldehyde **2i** (320 mg, 1.60 mmol). After purification by column chromatography on silica gel (CH_2Cl_2/EtOAc 9:1), the pure product (104 mg, 0.26 mmol) was obtained as a yellow solid. Yield, *50%*. m.p: 106 °C; ^{1}H NMR (300 MHz, DMSO-d_6) δ 7.55 (s, 1H), 7.53-7.48 (m, 3H), 7.43-7.37 (m, 3H), 7.32-7.26 (m, 2H), 6.82 (s, 1H), 5.42 (d, *J* = 4.8 Hz, 1H), 4.86-4.80 (m, 1H), 3.82 (s, 3H), 3.75 (s, 3H), 3.27-3.16 (m, 2H). ^{13}C NMR (75 MHz, DMSO-d_6) δ 159.0 (d, *J* = 244 Hz, 1C), 152.0, 146.9, 145.0, 141.6, 133.6, 130.6 (d, *J* = 3 Hz, 1C), 129.3 (d, *J* = 8 Hz, 1C), 128.4, 128.4, 128.3, 128.1 (d, *J* = 14 Hz, 1C), 126.0 (2C), 124.8 (d, *J* = 3 Hz, 1C), 116.0 (d, *J* = 22 Hz, 1C), 115.3, 107.8, 72.3, 55.9, 55.9, 42.3. HRMS (ESI+) m/z Calc. for $C_{22}H_{20}FNO_5$ $[M + Na]^+$ 420.1218, found 420.1214.

4.2.4.18. *2-(4,5-Dimethoxy-2-nitrophenyl)-1-(2'-nitro-[1,1'-biphenyl]-4-yl)ethanol* (**3r**). The crude product was prepared according to procedure **B** starting from **1** (74 mg, 0.32 mmol) and 2'-nitro-[1,1'-biphenyl]-4-carbaldehyde **2j** (220 mg, 0.97 mmol). After purification by column chromatography on silica gel (CH_2Cl_2/EtOAc 9:1), the pure product (58 mg, 0.14 mmol) was obtained as a light yellow solid. Yield, *44%*. m.p: 164 °C; ^{1}H NMR (300 MHz, DMSO-d_6) δ 7.96 (d, *J* = 7.9 Hz, 1H), 7.79-7.74 (m, 1H), 7.65-7.53 (m, 3H), 7.41 (d, *J* = 7.9 Hz, 2H), 7.30 (d, *J* = 7.9 Hz, 2H), 6.84 (s, 1H), 5.45 (d, *J* = 4.7 Hz, 1H), 4.86-4.80 (m, 1H), 3.83 (s, 3H), 3.78 (s, 3H), 3.25-3.17 (m, 2H). ^{13}C NMR (75 MHz, DMSO-d_6) δ 152.0, 148.9, 146.9, 145.5, 141.6, 135.4, 134.8, 132.7, 131.7, 128.7, 128.2, 127.4 (2C), 126.2 (2C), 123.9, 115.3, 107.9, 72.3, 55.9 (2C), 42.3. Anal. Calcd. for $C_{22}H_{20}N_2O_7$ (%): C, 62.26; H, 4.75; N, 6.60. Found (%): C, 62.21; H, 4.66; N, 6.47.

4.2.4.19. *2-(4,5-Dimethoxy-2-nitrophenyl)-1-(2'-(hydroxymethyl)-[1,1'-biphenyl]-4-yl)ethanol* (**3s**). The crude product was prepared according to procedure **B** starting from **1** (138 mg, 0.60 mmol) and 2'-(hydroxymethyl)-[1,1'-biphenyl]-4-carbaldehyde **2k** (380 mg, 1.79 mmol). After purification by column chromatography on silica gel (CH_2Cl_2/EtOAc 7:3), the pure product (124 mg, 0.31 mmol) was obtained as a light yellow solid. Yield, *51%*. m.p: 143 °C; ^{1}H NMR (300 MHz, DMSO-d_6) δ 7.59-7.57 (m, 1H), 7.55 (s, 1H), 7.40-7.30 (m, 6H), 7.21-7.19 (m, 1H), 6.85 (s, 1H), 5.40 (d, *J* = 4.7 Hz, 1H), 5.09 (t, *J* = 5.3 Hz, 1H), 4.86-4.80 (m, 1H), 4.41 (d, *J* = 5.3 Hz, 2H), 3.83 (s, 3H), 3.78 (s, 3H), 3.27-3.17 (m, 2H). ^{13}C NMR (75 MHz, DMSO-d_6) δ 152.0, 146.9, 144.1, 141.7, 139.9, 139.2, 139.0, 129.2, 128.6 (2C), 128.3, 127.9, 127.1, 126.7, 125.6 (2C), 115.3, 107.8, 72.4, 60.7, 55.9 (2C), 42.3. HRMS (ESI+) m/z Calc. for $C_{23}H_{23}NO_6$ $[M + Na]^+$ 432.1418, found 432.1418.

4.2.4.20. *3'-(2-(4,5-Dimethoxy-2-nitrophenyl)-1-hydroxyethyl)-[1,1'-biphenyl]-4-carbonitrile* (**3t**). The crude product was prepared according to procedure **B** starting from **1** (86 mg, 0.37 mmol) and 3'-formyl-[1,1'-biphenyl]-4-carbonitrile **2l** (230 mg, 1.11 mmol). After purification by column chromatography on silica gel (CH_2Cl_2/EtOAc 9:1), the pure product (75 mg, 0.19 mmol) was obtained as a light yellow solid. Yield, *50%*. m.p: 152 °C; ^{1}H NMR (250 MHz, DMSO-d_6) δ 7.94 (d, *J* = 8.2 Hz, 2H), 7.83 (d, *J* = 8.2 Hz, 2H), 7.64-7.60 (m, 2H), 7.54 (s, 1H), 7.49-7.36 (m, 2H), 6.86 (s, 1H), 5.50 (d, *J* = 4.8 Hz, 1H), 4.90-4.83 (m, 1H), 3.82 (s, 3H), 3.75 (s, 3H), 3.34-3.18 (m, 2H). ^{13}C NMR (100 MHz, DMSO-d_6) δ 152.0, 146.9, 146.4, 144.9, 141.7, 138.0, 132.9 (2C), 128.9, 128.3, 127.5 (2C), 126.2, 125.7, 124.5, 118.9, 115.3, 110.0, 107.8, 72.5, 55.9 (2C), 42.4. Anal. Calcd. for $C_{23}H_{20}N_2O_5$ (%): C, 68.31; H, 4.98; N, 6.93. Found (%): C, 68.39; H, 4.93; N, 6.73.

4.2.4.21. *1-(4'-Chloro-[1,1'-biphenyl]-3-yl)-2-(4,5-dimethoxy-2-nitrophenyl)ethanol* (**3u**). The crude product was prepared according to procedure **B** starting from **1** (82 mg, 0.35 mmol) and 4'-chloro-[1,1'-biphenyl]-3-carbaldehyde (230 mg, 1.06 mmol). After purification by column chromatography on silica gel (CH_2Cl_2/EtOAc 9:1), the pure product (56 mg, 0.13 mmol) was obtained as a yellow solid. Yield, *39%*. m.p: 81 °C; ^{1}H NMR (250 MHz, DMSO-d_6) δ 7.65 (d, *J* = 8.5 Hz, 2H), 7.57-7.51 (m, 5H), 7.45-7.39 (m, 1H), 7.33-7.30 (m, 1H), 6.86 (s, 1H), 5.47 (d, *J* = 4.9 Hz, 1H), 4.88-4.81 (m, 1H), 3.82 (s, 3H), 3.75 (s, 3H), 3.29-3.17 (m, 2H). ^{13}C NMR (75 MHz, DMSO-d_6) δ 152.1, 147.0, 146.2, 141.8, 139.3, 138.7, 132.4, 128.9 (2C), 128.8, 128.5 (2C), 128.4, 125.4, 125.3, 124.1, 115.4, 107.9, 72.7, 56.0 (2C), 42.4. Anal. Calcd. for $C_{22}H_{20}ClNO_5$ (%): C, 63.85; H, 4.87; N, 3.38. Found (%): C, 64.00; H, 4.79; N, 3.36.

4.2.4.22. *2-(4,5-Dimethoxy-2-nitrophenyl)-1-(4-(pyridin-4-yl)phenyl)ethanol* (**3v**). The crude product was prepared according to procedure **B** starting from **1** (109 mg, 0.47 mmol) and 4-(pyridin-4-yl)benzaldehyde **2m** (260 mg, 1.42 mmol). After purification by column chromatography on silica gel (CH_2Cl_2/EtOAc 6:4), the pure product (89 mg, 0.23 mmol) was obtained as a yellow solid. Yield, *50%*. m.p: 195 °C; ^{1}H NMR (250 MHz, DMSO-d_6) δ 8.62 (d, *J* = 5.8 Hz, 2H), 7.77 (d, *J* = 8.1 Hz, 2H), 7.70 (d, *J* = 5.8 Hz, 2H), 7.55 (s, 1H), 7.47 (d, *J* = 8.1 Hz, 2H), 6.87 (s, 1H), 5.50 (d, *J* = 4.9 Hz, 1H), 4.88-4.82 (m, 1H), 3.83 (s, 3H), 3.76 (s, 3H), 3.30-3.14 (m, 2H). ^{13}C NMR (100 MHz, DMSO-d_6) δ 152.0, 150.2 (2C), 146.9, 146.8, 146.7, 141.6, 135.7, 128.3, 126.6 (2C), 126.5 (2C), 121.1 (2C), 115.3, 107.8, 72.3, 56.0, 55.9,

42.4. Anal. Calcd. for $C_{21}H_{20}N_2O_5$ (%): C, 66.31; H, 5.30; N, 7.36. Found (%): C, 65.93; H, 5.32; N, 7.26.

4.2.4.23. *2-(4,5-Dimethoxy-2-nitrophenyl)-1-(4-(pyridin-3-yl)phenyl)ethanol* (**3w**). The crude product was prepared according to procedure **B** starting from **1** (81 mg, 0.35 mmol) and 4-(pyridin-3-yl)benzaldehyde **2n** (192 mg, 1.05 mmol). After purification by column chromatography on silica gel (CH_2Cl_2/EtOAc 6:4), the pure product (74 mg, 0.19 mmol) was obtained as a light yellow solid. Yield, *56%*. m.p: 164 °C; ^{1}H NMR (250 MHz, DMSO-d_6) δ 8.89 (d, *J* = 1.8 Hz, 1H), 8.56 (dd, *J* = 4.7, 1.4 Hz, 1H), 8.09-8.04 (m, 1H), 7.69 (d, *J* = 8.2 Hz, 2H), 7.55 (s, 1H), 7.50-7.44 (m, 3H), 6.87 (s, 1H), 5.47 (d, *J* = 4.9 Hz, 1H), 4.87-4.80 (m, 1H), 3.83 (s, 3H), 3.77 (s, 3H), 3.30-3.14 (m, 2H). ^{13}C NMR (100 MHz, DMSO-d_6) δ 152.0, 148.4, 147.6, 146.9, 145.5, 141.6, 135.7, 135.4, 134.0, 128.4, 126.6 (2C), 126.5 (2C), 123.9, 115.3, 107.8, 72.3, 56.0, 55.9, 42.4. HRMS (ESI+) m/z Calc. for $C_{21}H_{20}N_2O_5$ $[M + H]^+$ 381.1445, found 381.1446.

4.2.4.24. *2-(4,5-Dimethoxy-2-nitrophenyl)-1-(4-(thiophen-2-yl)phenyl)ethanol* (**3x**). The crude product was prepared according to procedure **B** starting from **1** (101 mg, 0.44 mmol) and 4-(thiophen-2-yl)benzaldehyde **2o** (246 mg, 1.31 mmol). After purification by column chromatography on silica gel (CH_2Cl_2/EtOAc 9:1), the pure product (92 mg, 0.24 mmol) was obtained as a light yellow solid. Yield, *55%*. m.p: 144 °C; ^{1}H NMR (250 MHz, DMSO-d_6) δ 7.62 (d, *J* = 8.2 Hz, 2H), 7.55 (s, 1H), 7.53 (dd, *J* = 5.1, 0.9 Hz, 1H), 7.49 (dd, *J* = 3.7, 0.9, 1H), 7.35 (d, *J* = 8.2 Hz, 2H), 7.13 (dd, *J* = 5.1, 3.7 Hz, 1H), 6.85 (s, 1H), 5.44 (d, *J* = 4.8 Hz, 1H), 4.83-4.76 (m, 1H), 3.83 (s, 3H), 3.76 (s, 3H), 3.28-3.13 (m, 2H). ^{13}C NMR (75 MHz, DMSO-d_6) δ 152.0, 146.9, 144.8, 143.3, 141.6, 132.4, 128.4, 128.2, 126.5 (2C), 125.3, 125.0 (2C), 123.4, 115.3, 107.8, 72.2, 55.9 (2C), 42.2. Anal. Calcd. for $C_{20}H_{19}NO_5S$ (%): C, 62.32; H, 4.97; N, 3.63; S, 8.32. Found (%): C, 61.97; H, 4.91; N, 3.63; S, 8.11.

4.2.4.25. *2-(4,5-Dimethoxy-2-nitrophenyl)-1-(4-(furan-3-yl)phenyl)ethanol* (**3y**). The crude product was prepared according to procedure **B** starting from **1** (64 mg, 0.28 mmol) and 4-(furan-3-yl)benzaldehyde **2p** (143 mg, 0.83 mmol). After purification by column chromatography on silica gel (CH_2Cl_2), the pure product (43 mg, 0.12 mmol) was obtained as a yellow solid. Yield, *43%*. m.p: 133 °C; ^{1}H NMR (250 MHz, DMSO-d_6) δ 8.16 (s, 1H), 7.74-7.73 (m, 1H), 7.55 (d, *J* = 8.1 Hz, 1H), 7.54 (s, 1H), 7.31 (d, *J* = 8.1 Hz, 1H), 6.95-6.94 (m, 1H), 6.84 (s, 1H), 5.39 (d, *J* = 4.8 Hz, 1H), 4.80-4.73 (m, 1H), 3.82 (s, 3H), 3.75 (s, 3H), 3.26-3.12 (m, 2H). ^{13}C NMR (100 MHz, DMSO-d_6) δ 152.0, 146.9, 144.2, 144.1, 141.6, 139.1,

130.6, 128.4, 126.2 (2C), 125.7, 125.2 (2C), 115.3, 108.7, 107.8, 72.4, 55.9 (2C), 42.4. Anal. Calcd. for $C_{20}H_{19}NO_6$ (%): C, 65.03; H, 5.18; N, 3.79. Found (%): C, 65.03; H, 5.08; N, 3.75.

Acknowledgments

This work was supported by the Centre National de la Recherche Scientifique. We express our thanks to Youssef Kabri, and Omar Khoumeri which were an enormous help in my everyday work and to Vincent Remusat for ^{1}H and ^{13}C NMR spectra recording. The antiviral work was performed by Els Scheers, Ph.D. in Rega Institute for Medical Resaerch.

References

[1] P. Simmonds, C. McIntyre, C. Savolainen-Kopra, C. Tapparel, I.M. Mackay, T. Hovi, Proposals for the classification of human rhinovirus species C into genotypically assigned types, *J. Gen. Virol.*, (2010), 91, 2409 - 2419.

[2] A.C. Palmenberg, D. Spiro, R. Kuzmickas, S. Wang, A. Djikeng, J.A. Rathe, C.M. Fraser-Liggett, S.B. Liggett, Sequencing and analyses of all known human rhinovirus genomes reveal structure and evolution, *Science*, (2009), 324, 55-59.

[3] E. Arunda, A. Pitkäranta, T.J. Witek, C.A. Doyle, F.G. Hayden, Frequency and natural history of rhinovirus infections in adults during autumn, *J. Clin. Microbiol.*, (1997), 35, 2864-2868.

[4] (a) V. Peltola, M. Waris, R. Österback, P. Susi, T. Hyypiä, O. Ruuskanen, Clinical effects of rhinovirus infections, *J. Clin. Virol*., (2008), 43, 411-414. (b) R.B. Turner, Rhinovirus: More than just a common cold virus, *J. Infect. Dis*., (2007), 195, 765-766. (c) E.K. Miller, N. Khuri-Bulos, J.V. Williams, A.A. Shehabi, S. Faouri, I. Al Jundi, Q. Chen, L. Heil, Y. Mohamed, L.L. Morin, A. Ali, N.B. Halasa, Human Rhinovirus C associated with wheezing in hospitalized children in the middle east, *J. Clin. Virol.*, (2009), 46, 85-89.

[5] A. Papi, M. Contoli, Rhinovirus vaccination: the case against, *Eur. Respir. J.*, (2011), 37, 5-7.

[6] (a) D.A. Shepard, B.A. Heinz, R.R. Rueckert, WIN 52035-2 inhibits both attachment and eclipse of Human Rhinovirus 14, *J. Virol*., (1993), 67, 2245-2254. (b) P.S. Dragovich, S.E. Webber, R.E. Babine, S.A. Fuhrman, A.K. Patick, D.A. Matthews, S.H. Reich, J.T. Marakovits, T.J. Prins, R. Zhou, J. Tikhe, E.S. Littlefield, T.M. Bleckman, M.B. Wallace, T.L. Little, C.E. Ford, J.W.III Meador, R.A. Ferre, E.L. Brown, S.L. Binford, D.M. DeLisle, S.T. Worland, Structure-based design, synthesis and biological evaluation of irreversible Human Rhinovirus 3C Protease inhibitors. 2. Peptide Structure-Activity studies, *J. Med.*

Chem., (1998), 41, 2819-2834. (c) M.J. Tebbe, W.A. Spitzer, F. Victor, S.C. Miller, C.C. Lee, T.R. Sattelberg, Sr, E. McKinney, J.C. Tang, Antirhino/enteroviral vinylacetylene benzimidazoles: a study of their activity and oral plasma levels in mice, *J. Med. Chem*., (1997), 40, 3937-3946. (d) S.E. Webber, J. Tikhe, S.T. Worland, S.A. Fuhrman, T.F. Hendrickson, D.A. Matthews, R.A. Love, A.K. Patick, J.W. Meador, R.A. Ferre, E.L. Brown, D.M. DeLisle, C.E. Ford, S.L. Binford, Design, synthesis, and evaluation of nonpeptidic inhibitors of Human Rhinovirus 3C protease, *J. Med. Chem*., (1996), 39, 5072-5082. (e) J.N. Lambert, The Biota Research and Product Development Team. BTA798 is an orally bioavailable and potent inhibitor of human rhinovirus both *in vitro* and in an experimental challenge virus infection model in healthy volunteers. In: Abstracts of the Fifty-first Interscience Conference on Antimicrobial Agents and Chemotherapy, Chicago, IL, (2011). Abstract V-1557. American society for Microbiology, Washington, DC, USA. (f) S. Feil, S. Hamilton, G.Y. Krippner, B. Lin, A. Luttick, D.B. McConnell, R. Nearn, M.W. Parker, J. Ryan, P.C. Stanislawski, S.P. Tucker, K.G. Watson, C.J. Morton, An orally available 3-ethoxybenzisoxazole capsid binder with clinical activity against Human Rhinovirus, *ACS Med. Chem. Letts*, (2012), *3*, 303-307.

[7] (a) P. Mallia, S.D. Message, V. Gielen, M. Contoli, K. Gray, T. Kebadze, J. Aniscenko, V. Laza-Stanca, M.R. Edwards, L. Slater, A. Papi, L.A. Stanciu, O.M. Kon, M. Johnson, S.L. Johnston, Experimental Rhinovirus infection as a human model of chronic obstructive pulmonary disease exacerbation, *Am. J. Respir. Crit. Care Med*., (2011), 183, 734-742. (b) D.J. Jackson, S.L. Johnston, The role of viruses in acute exacerbations of asthma, *J. Allergy Clin. Immunol*., (2010), 125, 6, 1178-1187.

[8] (a) J.L. Kennedy, R.B. Turner, T. Braciale, P.W. Heymann, L. Borish, Pathogenesis of rhinovirus infection, *Curr. Opin. Virol*., (2012), 2, 1-7. (b) J.M. Rollinger, T.M. Steindl, D. Schuster, J. Kirchmair, K. Anrain, E.P. Ellmerer, T. Langer, H. Stuppner, P. Wutzler, M. Schmidtke, Structure-based virtual screening for the discovery of natural inhibitors for Human Rhinovirus coat protein, *J. Med. Chem*., (2008), 51, 842-851. (c) C. Conti, N. Desideri, Synthesis and antirhinovirus activity of new 3-benzyl chromene and chroman derivatives, *Bioorg. Med. Chem*., (2009), 17, 3720-3727 (d) N. Falah, S. Violot, D. Décimo, F. Berri, M.L. Foucault-Grunenwald, T. Ohlmann, I. Schuffenecker, F. Morfin, B. Lina, B. Riteau, J.C. Cortay, *Ex vivo* and *in vivo* inhibition of Human Rhinovirus replication by a new pseudosubstrate of viral 2A protease, *J. Virol*., (2012), 86, 2, 691-704. (e) C. Lacroix, S. Laconi, F. Angius, A. Coluccia, R. Silvestri, R. Pompei, J. Neyts, P. Leyssen, *In vitro*

characterization of pleconaril/pirodavir-like compound with potent activity against rhinoviruses, *Virol J*., (2015), 12, 106-112.

[9] M.A. McKinlay, D.C Pevear, M.G. Rossman, Treatment of the picornavirus common cold by inhibitors of viral uncoating and attachment. *Annu. Rev. Microbiol*., (1992), 46, 635-654.

[10] (a) A.M. De Palma, I. Vliegen, E. De Clercq, J. Neyts, Selective inhibitors of Picornavirus replication, *Medicinal Research Reviews*, (2008), 6, 823-884. (b) V.A. Makarov, H. Braun, M. Richter, O.B. Riabova, J. Kirchmair, E.S. Kazakova, N. Seidel, P. Wutzler, M. Schmidtke, Pyrazolopyrimidines: Potent inhibitors targeting the capsid of Rhino- and Enteroviruses, *ChemMedChem*, (2015), 10, 1629-1634. (c) V.E. Kuz'min, A.G. Artemenko, E.N. Muratov, I.L. Volineckaya, V.A. Makarov, O.B. Riabova, P. Wutzler, M. Schmidtke, Quantitative structure-activity relationship studies of [(biphenyloxy)propyl]isoxazole derivatives. Inhibitors of Human Rhinovirus 2 replication, *J. Med. Chem*., (2007), 50, 4205-4213.

[11] M. Roche, C. Lacroix, O. Khoumeri, D. Franco, J. Neyts, T. Terme, P. Leyssen, P. Vanelle, Synthesis, biological activity and structure-activity relationship of 4,5-dimethoxybenzene derivatives inhibitor of rhinovirus 14 infection, *Eur. J. Med. Chem*., (2014), 76, 445-459.

[12] M. Mahesh, J.A. Murphy, F. LeStrat, H.P. Wessel, Reduction of arenediazoniumsalts by tetrakis(dimethylamino)ethylene (TDAE): efficient formation of products derived from aryl radical, *Beilstein J. Org. Chem*, (2009), 5, 1.

[13] J. Broggi, T. Terme, P. Vanelle, Organic electron donors as powerful single-electron reducing agents in organic synthesis, *Angew. Chem. Int. Ed.*, (2014), 53, 384-413.

[14] (a) G. Giuglio-Tonolo, T. Terme, M. Medebielle, J. Dolbier, Nucleophilic trifluoromethylation of acyl chlorides using the trifluoromethyl iodide/TDAE reagent, *Tetrahedron Lett.*, (2002), 43, 4317-4319. (b) O. Amiri-Attou, T. Terme, P. Vanelle, Functionalization of 6-nitrobenzo[1,3]dioxole with carbonyl compounds via TDAE methodology, *Molecules*, (2005), 10, 545-551. (c) M. Montana, T. Terme, P. Vanelle, Original synthesis of oxiranes via TDAE methodology: reaction of 2,2-dibromomethylquinoxaline with aromatic aldehydes, *Tetrahedron Lett.*, (2005), 46, 8373-8376. (d) M. Montana, T. Terme, P. Vanelle, Original synthesis of α-chloroketones in azaheterocyclic series using TDAE approach, *Tetrahedron Lett*., (2006), 47, 6573-6576. (e) M. Since, T. Terme, P. Vanelle, Original TDAE strategy using α-halocarbonyl derivatives, *Tetrahedron*, (2009), 65, 6128-6134. (f) O. Khoumeri, G. Giuglio-Tonolo, M.D. Crozet, T. Terme, P. Vanelle, Original synthesis of 2-substituted-4,11-dimethoxy-1-(phenylsulfonyl)-

2,3-dihydro-1*H*-naphtho[2,3-*f*]indole-5,10-diones using TDAE and Cu-catalyzed reaction strategy, *Tetrahedron*, (2011), 67, 6173-6180. (g) O. Khoumeri, M. Montana, T. Terme, P. Vanelle, Rapid and efficient synthesis of 2-substituted-tetrahydropyrido[3,4-*b*]quinoxalines using TDAE strategy, *Tetrahedron Letters*, (2012), 53, 2410-2413. (h) M. Roche, T. Terme, P. Vanelle, Original TDAE strategy using propargylic chloride: rapid access to 1,4-diarylbut-3-ynol derivatives, *Molecules*, (2013), 18, 1540-154.

[15] C. Lacroix, J. Querol-Audí, M. Roche, D. Franco, M. Froeyen, P. Guerra, T. Terme, P. Vanelle, N. Verdaguer, J. Neyts, P. Leyssen, A novel benzonitrile analogue inhibits rhinovirus replication, *J. Antimicrob. Chem.*, (2014), 69, 2723-2732.

[16] (a) O. Korb, T. Stutzle, T.E. Exner, PLANTS: Application of ant colony optimization to structure-based drug design. In *Ant colony optimization and swarm intelligence*, Proceedings of the 5th International Workshop, ANTS 2006, Belgium. (b) M. Dorigo, L.M. Gambardella, M. Birattari, A. Martinoli, R. Poli, T. Stutzle (Eds), 2006, Lecture Notes in Computer Science, Series 4150, pp 247-258.

[17] (a) R.A. Ö Friesner, R.B. Murphy, M.P. Repasky, L.L. Frye, J.R. Greenwood, T.A. Halgren, P.C. Sanschagrin, D.T. Mainz, Extra Precision Glide: Docking and Scoring Incorporating a Model of Hydrophobic Enclosure for Protein-Ligand Complexes, *J. Med. Chem.*, (2006), 49, 6177-6196. (b) Small-Molecule Drug Discovery Suite 2015-3: Glide version 6.8, Schrödinger, LLC, New York, NY, (2015).

[18] G.M. Morris, R. Huey, W. Lindstrom, M.F. Sanner, R.K. Belew, D.S. Goodsell, A.J. Olson, Autodock4 and AutoDockTools4: automated docking with selective receptor flexibility, *J. Computational Chemistry*, (2009), 16, 2785-2791.

[19] B. Rosenwirth, D.A. Oren, E. Arnold, Z.L. Kis, H.J. Eggers, SDZ 35-682, a new picornavirus capsid-binding agent with potent antiviral activity, *Antiviral Res.*, (1995), 26, 65-82.

[20] [On line] http://www.rcsb.org/

[21] Y. Zhang, A.A. Simpson, R.M. Ledford, C.M. Bator, S. Chakravarty, G.A. Skochko, T.M. Demenczuk, A. Watanyar, D.C. Pevear, M.G. Rossmann, Structural and virological studies of the stages of virus replication that are affected by antirhinovirus compounds, *J. Virol.*, (2004), 78, 11061-11069.

[22] K.H. Kim, P. Willingmann, Z.X. Gong, M.J. Kremer, M.S. Chapman, I. Minor, M.A. Oliveira, M.G. Rossmann, K. Andries, G.D. Diana, F.J. Dutko, M.A. McKinlay, D.C. Pevear, A Comparison of the Anti-rhinoviral Drug Binding Pocket in HRV14 and HRV1A, *J. Mol. Biol.*, (1993), 230, 206-227.

ACCEPTED MANUSCRIPT

[23] M.S. Chapman, I. Minor, M.G. Rossmann, G.D. Diana, K. Andries, Human rhinovirus 14 complexed with antiviral compound R61837, *J. Mol. Biol.*, (1991), 217, 455-463.

[24] Molecular Operating Environment (MOE) version 2009.10; Chemical Computing Group Inc.: Montreal, Canada; http://www. chemcomp.com/.

[25] PyMOL version 1.2r1; DeLanoScientificLLC: SanCarlos, CA http://www.pymol.org/.

ACCEPTED MANUSCRIPT

ACCEPTED MANUSCRIPT

Highlights

VP1 crystal structure-guided exploration and optimization of 4,5-dimethoxybenzene-based inhibitors of rhinovirus 14 infection

1. Description of potent derivatives with HRV serotype 14 activity.
2. Use of docking experiments (*in silico* design) to focus the chemistry effort.
3. Presentation of Structure Activity Relationships with topological approach.
4. The synthesis is straightforward and mainly achieved by using TDAE.

ACCEPTED MANUSCRIPT